Analysis of diurnal, seasonal and annual variations of fair weather atmospheric potential gradient at reduced number concentration of condensation nuclei from long-term measurements at Świder, Poland

Izabela Pawlak[1], Anna Odzimek[1], Daniel Kępski[1], and José Tacza[1]

[1]Institute of Geophysics, Polish Academy of Sciences, Księcia Janusza 64, 01-452 Warsaw, Poland

Correspondence: Izabela Pawlak (izap@igf.edu.pl)

Abstract. The ground-level atmospheric potential gradient (PG) has been measured with a radioactive collector method in Stanisław Kalinowski Geophysical Observatory in Świder (52.12°N, 21.23°E), Poland, for several decades. Long-term measurements analysed previously revealed rather typical behaviour in the diurnal and seasonal variations of the PG of a land station controlled by pollution. Observation of the potential gradient at such a station usually show a maximum at local winter months which are mostly affected by anthropogenic pollution. The 1965–2005 series has been newly analysed to describe the Świder PG variations in greater detail, also in connection with an analysis of simultaneous measurements of condensation nuclei measured at 6, 12, 18 UT. An attempt is made to calculate the diurnal and seasonal variations at condensation nuclei number concentrations below $10000 \ cm^{-3}$. There is a decrease of the PG in the diurnal variation by up to 11 % in the winter, and no significant change in the summer. The reduction in the annual variation is 11-26 % with the biggest difference in February. In the summer months, this difference is negligible. Such differences can be predicted with a simplified model of electrical conductivity including the aerosol composition of water soluble and soot particles, the main components of continental aerosol. With this model we obtained changes in the conductivity and the PG in up to 30 % in the winter, and 6 % in the summer. Despite the efforts to minimise the aerosol effect on the PG, the character of the PG seasonal and annual variation preserves its character with a maximum in the Northern Hemisphere winter and the minimum in the summer.

1 Introduction

1.1 Diurnal and seasonal variation of GEC as deduced from the atmospheric electricity stations observations

The Global Atmospheric Electric Circuit (GEC) manifests itself in the atmospheric potential gradient (PG) observed at any location on the globe (Rycroft et al., 2000). Diurnal and seasonal variations of the PG are the earliest recognised changes of the PG (e.g., Witkowski, 1902; Israël, 1973a, b). It has been also early established that even in fair weather (FW) conditions the curves of the diurnal variation had different shapes depending on the location of stations, season and local conditions. At land stations a double oscillation was often observed in the PG variation, present in at least one (usually warm) season (Israël, 1973a). For example, at Kew, Uppsala, Tokyo the diurnal variation of the PG exhibits the double oscillations at any time of

the year while at Helsinki, Tortosa or Vassijaure it had the double oscillation only in the local summer. At polar stations and over the oceans a single oscillation is usually observed throughout the year and its character is unitary in Universal Time (UT) (Odzimek, 2019) which has been firstly recognised by Hoffmann (1924). The average fair weather variation of the PG calculated from 1920–1925 observations over the oceans on board of the Carnegie Institution of Washington research vessel "Carnegie" is known as the Carnegie curve (Parkinson and Torreson, 1931; Harrison, 2013). This curve is considered to reflect the variation of the diurnal activity of the global circuit and is often compared with the diurnal variation of the PG observed in fair weather conditions from other places on the globe (e.g., Kubicki et al., 2016; Nicoll et al., 2019; Tacza et al., 2020; Michnowski et al., 2021, and others). In the seasonal or annual variation many observations indicated a winter maximum in the atmospheric potential gradient compared to the summer. Adlerman and Williams (1996) investigated the connection between the PG local winter maximum and more intensive anthropogenic emission of Aitken nuclei which occurred independent of the station's location in Northern or Southern Hemispheres. The annual variation of the air conductivity which minimises during the local winter as compared to the summer supported this relationship.

A question arises then when the true maximum of the GEC is, and Adlerman and Williams (1996) argued this should be investigated based on observations in locations relatively free from aerosol particles effects. Their analysis of Mauna Loa air-Earth current data and reanalysis of Carnegie and Maud cruises PG data indicated a GEC maximum in the Northern hemisphere summer, in agreement with the maximum of global thunderstorm activity (Christian et al., 2003).

In this paper we reanalyse the diurnal, seasonal and annual variation in the atmospheric potential gradient at the land station Świder (Poland) which also has condensation nuclei monitoring. Previous analyses of the diurnal variation of the PG indicate that Świder is characterised by the double oscillation prevalent in the summer (Northern Hemisphere summer), and the single oscillation in the winter. Furthermore PG values in winter are of higher average amplitude, explained by the higher emissions of anthropogenic aerosols affecting the local electric conductivity (Warzecha, 1976; Kubicki et al., 2003, 2007; Michnowski et al., 2021). This is rather a typical behaviour of the PG at a rural land station (Israël, 1973a). Here we analyse the variations at possible low levels of the nuclei number concentration, i.e. less than 10000 particles in cubic centimetre, to investigate whether, with such a limit applied, this may have any considerable effect on the seasonal peaks of the PG. We choose concentrations below 10000 particles per cm^{-3} because these are characteristic for rural, non-urban and remote regions of the globe (e.g., Mohnen and Hidy, 2010).

2 Świder published data set of atmospheric electricity

Stanisław Kalinowski Geophysical Observatory of the Institute of Geophysics, Polish Academy of Sciences, is located 25 km south-west of Warsaw near the Otwock town in the central Poland (52.12°N, 21.23°E). It was founded as a Magnetic Observatory, and since 1929 also worked as an atmospheric electricity station except during the World War II. The pre-war electric measurements were lost, and publication of new results of resumed electric measurements started in 1958. Measurements reports from years 1957–2005 were subsequently published in the Observatory yearbooks (Warzecha, 1960, 1968; Kubicki, 2006). Since the beginning of the atmospheric electric measurements, the PG was the main variable to be measured. After 1949

the measurements were complemented by air conductivity recordings and in the 2000' by the Maxwell current density measurements. In this paper we analyse only PG data since it is the most commonly measured parameter of atmospheric electricity worldwide.

2.1 PG data

60 The measurements of fair weather atmospheric potential gradient (or the atmospheric electric field strength) at the Świder observatory have been made with radioactive collectors (the activity of about 30 μCi). Initially two independent collectors were used, each consisting of the radioactive sonde at a height of about 2 m connected to an electrometer and a recording milliammeter. At the beginning Benndorf electrometers were used, in 1964 replaced by an observatory-built electrometer (Warzecha, 1968, 1976). After 2000 it was replaced by commercially available electrometers. The recording milliammeter was

65 also later replaced by an A/D logger. The PG measurements have absolute calibration and reduction to free plane value (e.g., Kubicki, 2006, and earlier yearbooks). The hourly averages of the PG measured with the collector as well as the positive air conductivity data were published in the observatory yearbooks for the period 1957–2005. The list of all yearbooks used in this study can be found in Appendix A.

2.2 Condensation nuclei data

70 Since the continuous atmospheric electricity observations simultaneous systematic measurements of aerosol particle number concentrations of the condensation nuclei type (CN, particle size from 0.005 μm to 10 μm) were made (Warzecha, 1960, 1974). The measurements have been made at a height of 1 m, three times a day at about 6, 12 and 18 UT. From 1957 to 1981 a small Scholz counter has been used for this purpose and since 1982 an observatory-built photoelectric counter (Kubicki et al., 2003). Only during 1998–1999 the measurements have been taken at 3 m height. The measurements of the concentration of

75 condensation nuclei at the three terms have been included in the observatory yearbooks.

2.3 Criteria of fair weather conditions

In order to investigate global signal of atmospheric electricity and minimise the effects of local weather, criteria for fair weather conditions are used (Imyanitov and Chubarina, 1967). Since 1965 a WMO standard for the fair-weather conditions has been applied at Świder: low cloudiness up to 3/8 in okta scale, no precipitation or fog, wind speed less than 6 m/s and PG amplitude

80 less than 1000 V/m (e.g., Warzecha, 1968; Kubicki, 2006).

3 Overview of fair-weather PG and CN data

In our analysis we consider all fair weather (FW) hourly values of the potential gradient (PG) and the condensation nuclei concentrations (CN) from 6, 12, 18 UT published in the Observatory yearbooks 1965–2005. There is a total number of the hourly PG values of 131634 with a subset of 16072 hourly values with corresponding CN concentrations and 3303 missing

85 data (2.5 %). Table B1 and Table B2 in the Appendix B include the number of FW hourly average mean values of PG and

number of FW days (24 h) for each month and year of the analysed period. There are more FW values during the local warmer seasons from March to September. The percentage of FW hours is about 37 % on average (see also Table 1) and varies between 49 % in the summer and 23 % during winter. The total number of FW days is equal to 1414. The percentage of FW days is about 9 % on average and rises to 14 % during summer and decreases to 4 % during winter.

Time series of monthly values of fair weather PG and CN
SWI 1965-2005 yearbook data
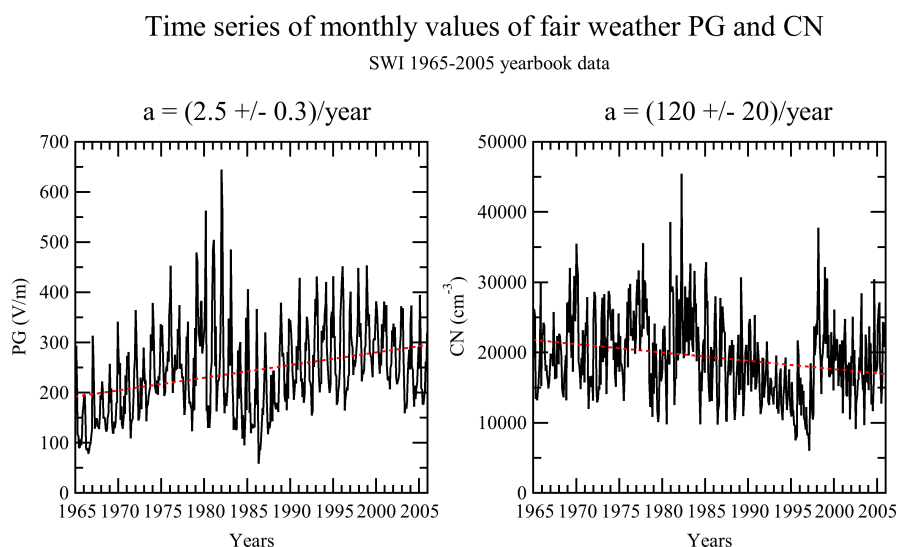
Figure 1. Time series of monthly averaged values of fair-weather PG and CN values over January 1965 – December 2005. The dashed red lines indicate positive trend for PG (2.5±0.3 V/m per year) and negative trend for CN (–120±20 cm^{-3}).

The time variations of monthly mean values of PG and CN during this period is shown in Fig. 1. There seems to be several periods of monotonic increase and decrease of the PG, and a general trend of increase of the PG by 2.5 V/m per year. The general trend for CN concentration is a decrease by –120±20 cm^{-3} per year. Analysis of the long-term variation in these series will be a subject of another study.

Histogram of these values and main statistical parameters of the set are given in Fig. 2. The mean average, Ma, of the total fair-weather PG of 1965–2005 is 230 V/m, and the standard deviation, SD, is 131 V/m. The median, Me, is 207 V/m, the first quartile, Q1, equals 139 V/m, and the third quartile, Q3, 294 V/m. The kurtosis, K, is equal to 5.4 and the skewness, S, is 1.3 what characterises a leptokurtic and right-skewed distribution. These parameters describe the total FW PG set but in next sections we concentrate on the subset of PG hours for which simultaneously measured CN data also exist, and particularly on the subset for limited CN concentrations up to 10000 cm^{-3}. The statistical parameters of the distribution of these subsets are also given in Fig. 2 separated by slashes. The selection of PG data measured at the same time as CN creates a new distribution with slightly higher mean (248 V/m) or median value (224 V/m) but similar kurtosis and skewness of ∼5 and ∼1, respectively. When we further limit the CN concentration the mean and median value are lower, 221 V/m and 208 V/m, respectively.

Selection of PG-CN pairs limits the number of values, N, to 16072 (12 %) and with the condition of CN lower than 10000 cm^{-3} the number of pairs decreases to 3593 (3 %) as indicated in the Table 1.

Table 1. Number of total hours for the period January 1965 – December 2005 together with number of all fair-weather PG hours and number of fair-weather PG hours corresponding to the CN concentration values below 10000 cm^{-3}, 8000 cm^{-3}, 6000 cm^{-3} and 4000 cm^{-3}, respectively. The percentages refer to the number in bold in the same colour in the first raw of the table.

All hours 1965-2005	All FW hours 1965-2005	FW PG hours 1965-2005	FW PG all CN	FW PG CN<10000	FW PG CN<8000	FW PG CN<6000	FW PG CN<4000
359400	**134937**	**131634**	**16072**	**3593**	**2025**	**915**	**122**
	37.54 %	97.5 %	4.47 %	1.00 %	0.56 %	0.25 %	0.03 %
			11.91 %	2.66 %	1.50 %	0.69 %	0.09 %
			12.21 %	2.72 %	1.54 %	0.71 %	0.09 %
				22.35 %	12.60 %	5.69 %	0.76 %
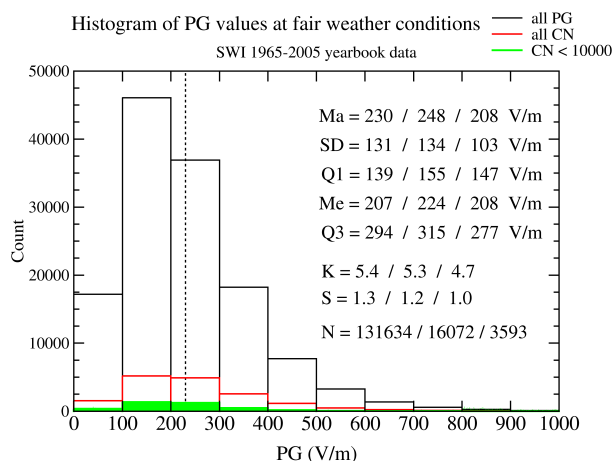
Figure 2. Histogram of the PG values measured during fair-weather conditions in January 1965 – December 2005: black colour – all PG values, red colour – PG values recorded simultaneously with CN concentrations, green colour – the PG values at CN concentrations below 10000 cm^{-3}. The black dashed line represents mean PG value (230 V/m). The other statistical parameters separately for the three PG groups are given in the legend, including the number of data values, N.

In Fig. 3 we show the histogram of the measured CN values. The mean value of the total fair-weather CN concentration is 18980 cm^{-3} and the standard deviation is 13240 cm^{-3}. The median is 15510 cm^{-3}, the first quartile is 10340 cm^{-3} and the third quartile is 22650 cm^{-3}. The kurtosis is equal to 8.8 and the skewness 2.1 what indicates a leptokurtic and right-skewed distribution. The number of fair-weather CN values is 16756 and the subset of CN below 10000 cm^{-3} (see green frame in

Fig. 3) is 3736 which corresponds to 22 % of the total CN values. Table 2 and Fig. 4 show the main statistical measures of the

110 FW PG and CN distributions discussed above and separately for each season. Fig. 4 presents the seasonal distribution of CN

concentrations. The green line separates the distributions of CN concentrations below 10000 cm^{-3} which will be used in next

sections.
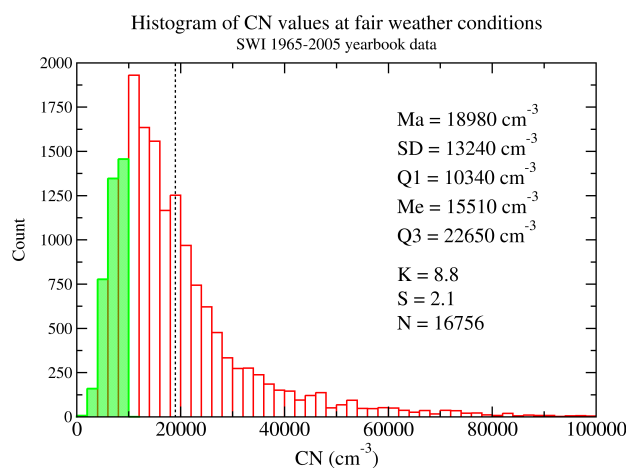
Figure 3. Histogram of hourly averaged CN concentrations at fair–weather conditions in January 1965 – December 2005: CN below 10000 cm^{-3} are framed in green, red colour – all CN. The black dashed line represents mean CN concentration value of 18980 cm^{-3}.

Table 2. Statistical measures of the distribution of all values FW PG and CN in the series 1965-2005.

	Spring		Summer		Autumn		Winter		all year	
	PG	CN	PG	CN	PG	CN	PG	CN	PG	CN
	(V/m)	(cm^{-3})	(V/m)	(cm^{-3})	(V/m)	(cm^{-3})	(V/m)	(cm^{-3})	(V/m)	(cm^{-3})
mean	250	21180	193	15330	253	20020	351	20930	249	18970
sd	129	14940	84	11220	130	12970	165	12800	134	13270
skewness	1.2	1.9	0.8	2.9	1.0	1.9	0.6	1.7	1.2	2.1
kurtosis	5.7	7.0	4.8	15.2	4.7	7.9	3.2	7.4	5.3	8.8

The lowest concentrations of CN in fair weather conditions (there is almost twice more counts of the concentrations in the

summer compared to winter) are observed in the summer with the mean value of ∼15000 cm^{-3}. In the other seasons the mean

115 value is close to 20000 cm^{-3} with the highest standard deviation values in the spring ∼15000 cm^{-3} and the lowest ∼11000

cm^{-3} in the summer and ∼13000 cm^{-3} in the winter and in the autumn. In terms of kurtosis and skewness the values in the

spring, autumn and winter are similar and vary between 7.0-7.9 and 1.7-1.9, respectively. In the summer these parameters are

higher reaching values 15.2 and 2.9, respectively.
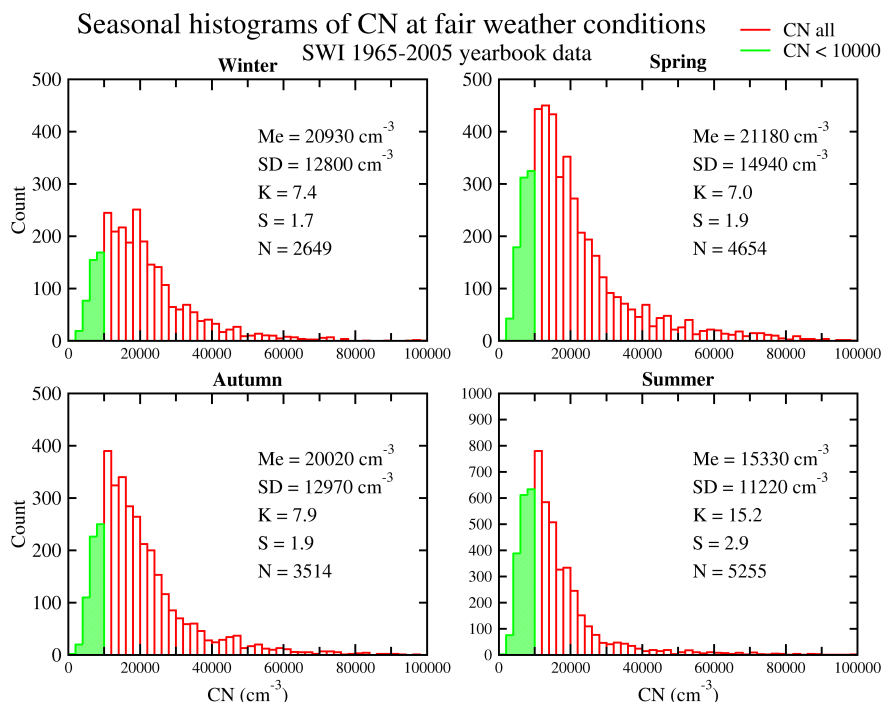
Figure 4. Seasonal histograms of the hourly averaged (6, 12, 18 UT) CN concentration values measured during fair weather conditions for the period January 1965 – December 2005: red colour – all CN concentration values, green colour – CN concentration values below 10000 cm^{-3}. Note that Y–axis ranges for summer (0-1000 counts) is twice compared with the other seasons (0-500 counts).

4 Diurnal and seasonal variation of the potential gradient in Świder, 1965-2005

In this section we analyse the diurnal and seasonal variation of Świder FW PG and how it relates to different levels of CN concentrations. Previous works on the analysis of diurnal and seasonal variations of PG focused only in FW days which considered 24 hours of FW, i.e., a FW day needed to accomplished FW for each hour between 0 and 23 UT concerned only of 24h fair weather days (Kubicki et al., 2016). This restriction limited the amount of available data. Michnowski et al. (2021) used FW PG values with at least 12 hours of fair weather conditions. In this work we increase the amount of data taking in account every FW hourly value to calculate the diurnal and seasonal variation.

4.1 Diurnal variation

Fig. 5 presents the PG diurnal variation separated by seasons (winter – December, January, February, spring – March, April, May, summer – June, July, August, autumn – September, October, November) and all year mean. The shape of the PG curve is substantially different depending on the season. During the winter months there is a single broad maximum lasting from the noon (~13 UT) until late evening (~20 UT) whereas during the spring-summer-autumn period double maxima (~7 and ~19 UT) are present. The amplitude variation of the PG curve during the winter is larger than in the summer (Table 2). Świder

is thus characterised by the type I of the "double oscillation" variation in the diurnal average curve as according to Israël (1973a), i.e. the double oscillation is prevalent except of local wintertime and its maxima occur at different hours depending on the season. Differences between the PG diurnal curves, at Świder, and the classical Carnegie diurnal curve, the "single

135   oscillation" and unitary variation in universal time – which is observed over the oceans and polar regions – come from the much greater variability and dynamics of the planetary boundary layer (PBL) characteristic for the location and at Świder affected by pollution, meteorological factors and seasonal effects (Kubicki et al., 2016; Nicoll et al., 2019; Michnowski et al., 2021, Section 4).
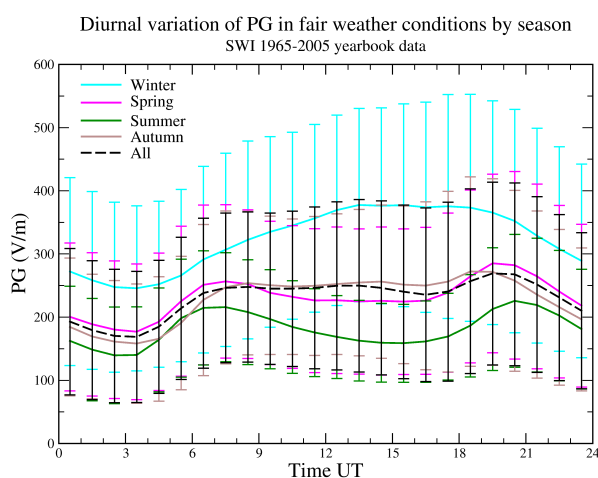
Figure 5. Diurnal variation of PG measured during fair–weather conditions by seasons and for the whole year in January 1965 – December 2005. The error bars represent ±1 standard deviation.

Since we cannot calculate the whole diurnal variation of CN we show results only for 6, 12, 18 UT (represented by symbols)

140   in Fig. 6. On the background (solid lines) is shown the Świder diurnal curves 1968/69 from Warzecha (1976), obtained from the recordings of the condensation nuclei concentrations using a Verzár counter every 15 minutes. We note that in this comparison we calculated the mean values only for 24-hour FW days since Warzecha presented the diurnal curves for cloudless days. The mean CN values for the seasons are given in the Table 2. The highest mean CN concentrations at these hours are registered at 12 UT although looking at diurnal curves of Warzecha (1976) this is already after the morning maximum of CN concentrations

145   between 6 and 12 UT (all seasons) and before the afternoon/evening maximum. These values are especially high in winter and spring 1968/69. The values at 6 and 18 UT are similar, however the lowest values are noted in the morning. At 6 and 18 UT the mean CN concentrations in the spring and autumn are almost equal while at 12 UT the spring mean is higher, even than the winter value which generally is the highest among seasons. Compared with the diurnal curves of Warzecha (1976) the CN concentrations fairly agree with the diurnal variation except for the 18 UT (excluding summer) and for 12 UT in summer and

150   autumn. Some differences are likely since we compare long-term mean values with one year means. Nevertheless, it is worth noting that the diurnal CN curves fall between the CN averages at one standard deviation.
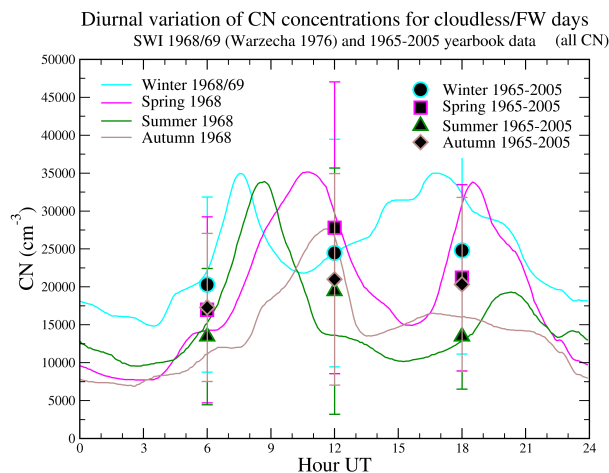
Figure 6. Diurnal variation of CN concentration values for cloudless days in spring 1968 – winter 1968/1969 and mean CN concentrations measured for 6, 12, 18 UT in 1965–2005.

4.2 Seasonal and annual variation

Analogically to Fig. 4 in Fig. 7 we show the seasonal differences in the distribution of FW PG at different CN concentrations. Their main statistical parameters for seasonal distributions are given in the figures as well as in Table 2. Fig. 7 presents the

155   seasonal histograms of the hourly averaged (at 6, 12, 18 UT) FW PG values for 1965–2005. Each histogram contains two types of distributions: red colour indicates the FW PG values measured simultaneously with CN concentrations, and green colour indicates a subset of the FW PG values for CN concentrations less than 10000 cm^{-3}. The main statistical measures for both of these distributions are displayed within each plot. Depending on the season we observe different PG distribution characteristics. For spring, summer and autumn most values ranged between 100-300 V/m with mean value of ∼250 V/m in

160   the spring and autumn and ∼200 V/m in the summer. Winter values ranged between 200–400 V/m and the mean was ∼350 V/m. The standard deviation is also the highest in the winter. The kurtosis values during spring and autumn are 4.7-4.8 while the summer kurtosis is the highest at 5.7 and the winter is the lowest at 3.2. The skewness of the winter distribution is the lowest of 0.6, and the skewness of all the other distributions is between 0.8-1.2 indicating more values concentrated around the mean value. Limiting the CN concentrations does not significantly change the distributions of corresponding PG values.

165   Another way to look at the relationship between aerosol or condensation nuclei concentration is presented in the Fig. 8. Intensity of colour indicates the number (counts) of data points at certain range of PG and CN. Here the PG values are plotted against CN concentrations by season. In the summer there seems to be little influence of CN concentration on PG as the similar range of PG values is observed at wide range of CN concentrations. Some kind of dependency is visible in the winter, and spring and autumn are intermediate in this manner with some high PG values at high CN concentrations.
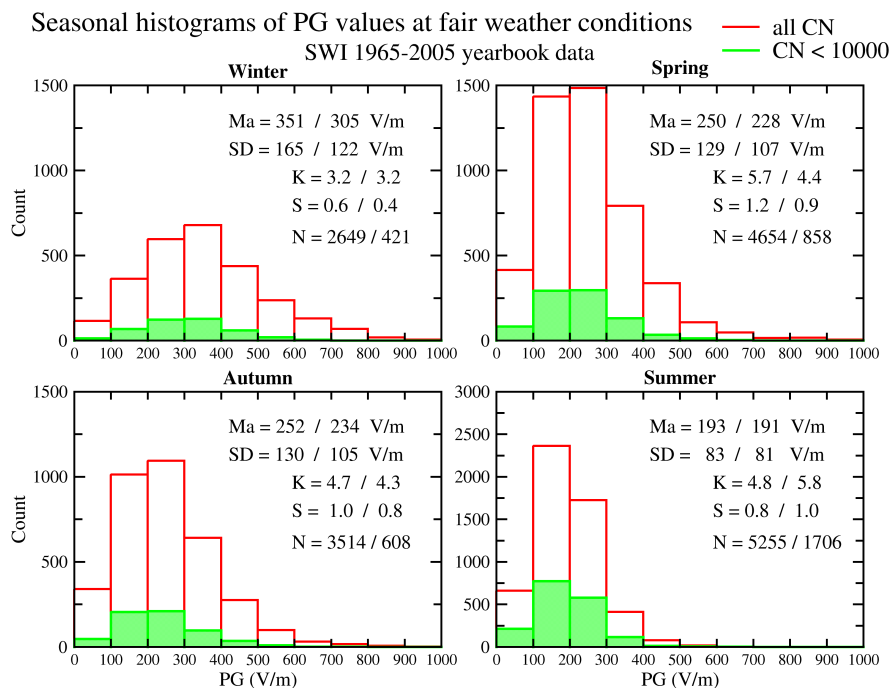
Figure 7. Seasonal histograms of the hourly averaged (6, 12, 18 UT) PG values measured during fair–weather conditions in January 1965 – December 2005: red colour–PG values measured simultaneously with all CN concentration values (6, 12, 18 UT), green colour–PG values measured simultaneously with CN concentrations below 10000 cm^{-3}. Note that the Y–axis ranges for summer (0-3000 counts) is twice compared with the other seasons (0-1500 counts).
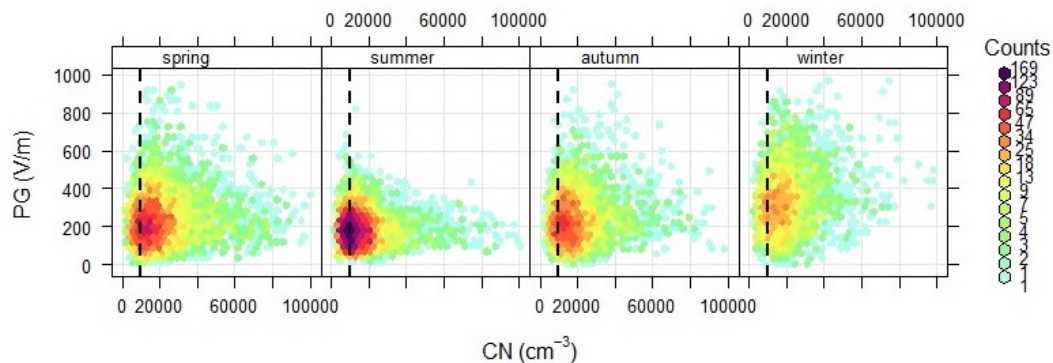
Figure 8. Seasonal dependence of hourly averaged values of fair–weather PG and CN concentration values in January 1965 – December 2005. Horizontal dashed line indicates the limit of CN concentration at 10000 cm^{-3}.

5 Diurnal, seasonal and annual variation at different level of CN concentration

Atmospheric potential gradient strictly depends on local conductivity of the air. The process of attaching of highly electrically ions to the aerosols causes reduction their mobility and, consequently, a decrease of local conductivity and an increase of the PG values (e.g., Israël, 1973a; Bennett and Harrison, 2008; Matthews et al., 2019; Wright et al., 2020). In this section we analyse if limiting CN concentrations to the lowest ranges in the CN distribution affects the PG values. We consider CN concentrations below 10000 cm^{-3} (green histograms in Fig. 4) and decrease the concentration limit by 2000 cm^{-3} (10000 cm^{-3}, 8000 cm^{-3}, 6000 cm-3) to investigate the diurnal, seasonal and annual variations of PG at the lowest CN concentrations. In earlier sections we showed that limiting the CN concentration to 10000 cm^{-3} did not change significantly the PG distributions, here we investigate if any possible extreme limits affect this behaviour. Right part of Table 1 presents the counts and percentages of the whole PG population of values within each CN concentration limit. In Fig. 9, in the upper panel we show the histograms of CN concentrations and in next panels are shown the histograms of PG values at the three selected limits of CN concentration. There are 3736 values below 10000 cm^{-3}, 2086 values below 8000 cm^{-3} and 939 values below 6000 cm^{-3}, which is about 23 %, 13 %, 6 % of all CN concentrations, respectively. Below 4000 cm^{-3} there was only 123 values (0.8 %) and therefore this subset was not taken into account. These values represent the whole span of the studied time period, as shown in the small panel in the top panel of Fig. 9. They also represent all seasons as shown in Table 6, even though there is proportionally more counts in the warmer season because of better FW conditions. In the lower panels of Fig. 9 the histograms of corresponding PG values are shown. We note a slightly decreasing tendency in the mean value of the population especially at CN concentrations below 6000 cm^{-3} approximately 210 V/m and lower kurtosis and skewness compared with the distributions below 10000 cm^{-3} and 8000 cm^{-3}.

Seasonal means are shown in Table 3 and Fig. 10 for each hour term (6, 12, 18 UT) and the mean average over the terms, together with the standard error of the mean. Here we also notice a decrease in the mean values of PG for each term at lower CN concentrations particularly at 6000 cm^{-3} limit (i.e., comparing PG values between CN-all and CN below 6000 cm^{-3}). This is present in the winter (73±15 V/m or ~13 % for total mean value), spring (30±8 V/m or ~12 %) and autumn (29±9 V/m or ~12 %) and the decrease are larger for 6 UT (e.g., 30±12 V/m or 12 % in the spring) and 18 UT (e.g., 57±29 V/m or 15 % in the winter, 36±23 V/m or 14 % in the spring). However, in the summer there is practically no effect of CN and no clear tendency of decrease or increase (the largest decrease of several V/m only).

Finally, in Fig. 11 and Table 4 the annual variation of FW PG is presented, calculated as monthly averages. Additionally in Table B3 in the Appendix B the number of FW PG values calculated as monthly values for all and limited CN concentration is presented. PG variations calculated at 6, 12, 18 UT are plotted separately from the average curve. The maximum of the PG is in February which is also the maximum at 12, 18 UT. The minimum of PG is in June which is also the month of the minimum at 6, 12 and 18 UT. The lowest PG amplitude of the differences between the maximum and the minimum are in the 6 UT curve: 91±12 V/m (wide maximum Dec-Mar, minimum in June) and much higher PG differences are at 12 and 18 UT: 213±12 V/m (Feb-Jun) and 217±13 V/m (Feb-Jun/Jul), respectively, 174±7 V/m (Feb-Jun) in the average curve.
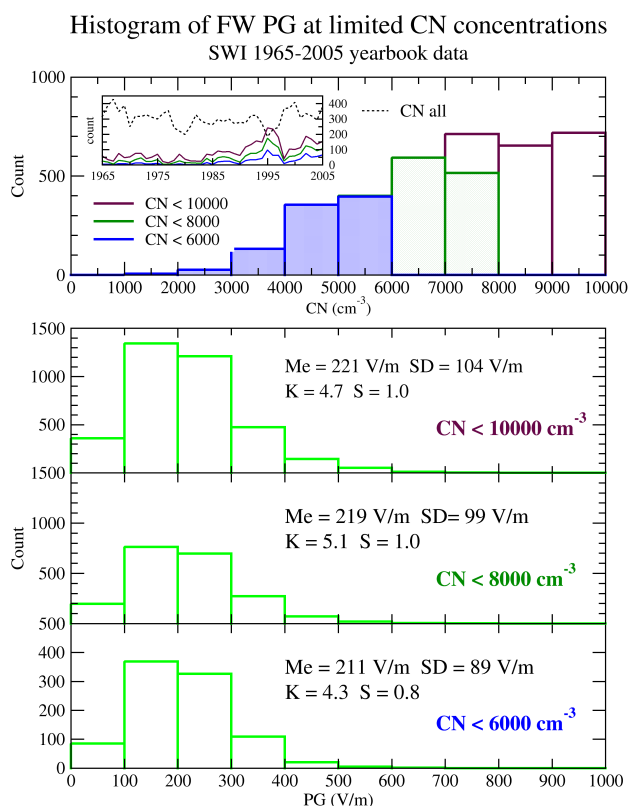
Figure 9. Histograms of the limited CN concentration values measured during fair–weather conditions divided into CN range: below 10000 cm^{-3} (purple), 8000 cm^{-3} (green), and 6000 cm^{-3} (blue), Bottom panels: histograms of hourly averaged PG values measured at limited CN concentration.

In the PG variations represented by the curves calculated with limitations of CN concentration there is a significant reduction of PG from October to March (11 %–26 %) and the biggest differences are seen in February at each term 6, 12, 18 UT and on average. In February the PG decreases by 95±25 V/m or 26 %. In January and November the change is about 20 % (75±24 V/m and 58±20 V/m, respectively) and in December about 13 % (45±28 V/m). From April to September there is a lack of or little influence of low CN concentration, and the PG differences are mostly of several V/m, which is of the order of the standard deviation of the mean error, except for April and September where these differences can be larger than 10 V/m. In September at 18 UT we note a larger decrease of PG of 44±29 V/m (18 %). In addition, as we already have seen in the seasonal plots in Fig. 10 at 12 UT there is even an inverse relationship between the PG and CN. For example in July at 12, 18 UT and in August at 18 UT, although these differences are within the statistical error. In terms of the change of the amplitude of maximum–minimum differences at 6 UT there is a small change with decreasing CN concentration reaching 77±41 V/m (Dec–Jun) at 6000 cm^{-3} CN limit. At 12 UT it is 165±35 V/m (Jan–Jul) at 6000 CN limit while at 10000 and 8000 CN limit it is practically the same as with no limits (∼213±12 V/m, Jan/Feb–Jun–Jul). At 18 UT at all CN limits the amplitude is ∼160

Table 3. Mean values of PG measured for fair–weather conditions by season for all and limited CN concentration values together with the one standard error of the mean corresponding to 6, 12, 18 UT and on average.

	Winter				Spring			
Hour	6 UT	12 UT	18 UT	Mean	6 UT	12 UT	18 UT	Mean
CN all	291 ± 6	370 ± 5	373 ± 6	350 ± 3	251 ± 3	227 ± 3	264 ± 3	250 ± 2
CN <10000	265 ± 9	339 ± 12	320 ± 10	305 ± 6	228 ± 5	217 ± 6	238 ± 7	228 ± 4
CN <8000	258 ± 12	333 ± 16	318 ± 13	299 ± 8	231 ± 7	219 ± 8	228 ± 11	227 ± 5
CN <6000	225 ± 15	342 ± 19	316 ± 23	277 ± 12	221 ± 9	215 ± 9	228 ± 20	220 ± 6

	Autumn				Summer			
Hour	6 UT	12 UT	18 UT	Mean	6 UT	12 UT	18 UT	Mean
CN all	227 ± 4	253 ± 3	272 ± 4	253 ± 2	215 ± 2	169 ± 2	187 ± 2	193 ± 1
CN <10000	210 ± 8	238 ± 6	261 ± 10	235 ± 4	207 ± 3	168 ± 3	188 ± 3	192 ± 2
CN <8000	213 ± 10	231 ± 7	256 ± 13	231 ± 5	208 ± 4	169 ± 4	194 ± 4	193 ± 2
CN <6000	208 ± 12	227 ± 9	242 ± 19	224 ± 7	202 ± 7	174 ± 5	196 ± 7	190 ± 3

215 V/m compared with 217±13 V/m with no limits. There seems to be slight shift between the maximum or minimum month which is January or February for the maximum, and June and July for the minimum. In general, there are significantly lower differences between winter and summer in the annual variation of the FW PG at the lowest CN concentration limit considered, however, the maximum still stays in the winter (Dec–Jan–Feb).

6   PG and conductivity model with variable aerosol content

220 In this section we model a hypothetical change in the PG when we limit the number concentration of CN. The relationship between atmospheric electric potential gradient and aerosol concentration is complex. These two most often measured variables are related through the electrical conductivity of the air. The conductivity, σ, is influenced by the loss of small atmospheric ions due to attachment to aerosol particles, and decreases when the attachment intensifies.

In fair weather the rate of the loss of ions is mainly due to the attachment to aerosol particles. The process of attachment

225 is dependent both on the number concentration and the spectrum of the size of aerosol particles, and is usually expressed by the ion-aerosol loss term, in general being a sum of contributions over different aerosol types and sizes (e.g., Israël, 1973a; Tinsley and Zhou, 2006). The term can be replaced by the effective coefficient β and the total aerosol concentration N, i.e. βN as in Eq. 1. The other parameters in Eq. 1 are: $q = 1$ cm$^3 s^{-1}$– ion production rate, $\alpha = 1.3 \times^{-7}$ cm^{-3} – the ion recombination coefficient, $\mu = 1.5$ cm$^2 V s^{-1}$ – the ion mobility and $e = 1.6 \times 10^{-19}$ C – the elementary electric charge. We assume that the

230 mobility and concentration of positive and negative ions are equal.
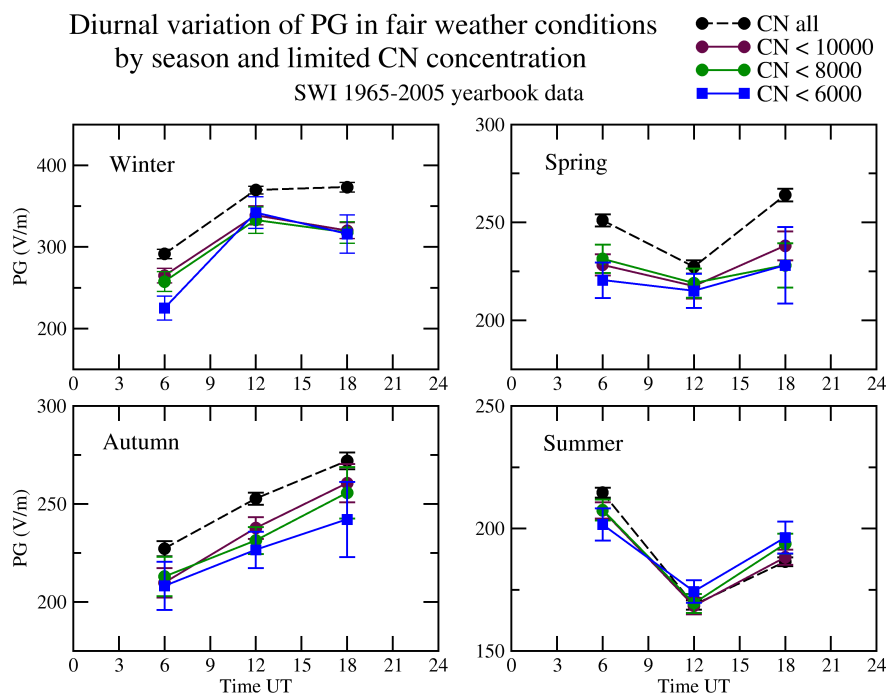
Figure 10. Diurnal variation of PG values measured during fair–weather conditions at 6, 12, 18 UT. divided into seasons, for the period January 1965 – December 2005 for all CN concentration values (black), and CN concentration values below: 10000 cm^{-3} (brown), 8000 cm^{-3} (green), 6000 cm^{-3} (blue). Error bars indicate one standard error of the mean.

$$\sigma = \frac{4e\mu q}{\beta N + \sqrt{(\beta N)^2 + 4\alpha q}} \qquad (1)$$

In case where the conduction current, $j_C = \sigma$ PG, is preserved, a decrease or increase in the electrical conductivity should
235   result in proportional increase or, respectively, decrease in the potential gradient:

$$\frac{\sigma_2}{\sigma_1} = \frac{PG_1}{PG_2} = s \qquad (2)$$

where indices 1 and 2 refer to value before and after the change, respectively.
240   According to Kubicki et al. (2016), rural continental aerosols of natural origin occurs in Świder, but there is also a lot of pollution from suburban traffic and domestic heating (Majewski and Przewoźniczuk, 2009; Pietruczuk and Jarosławski, 2013).
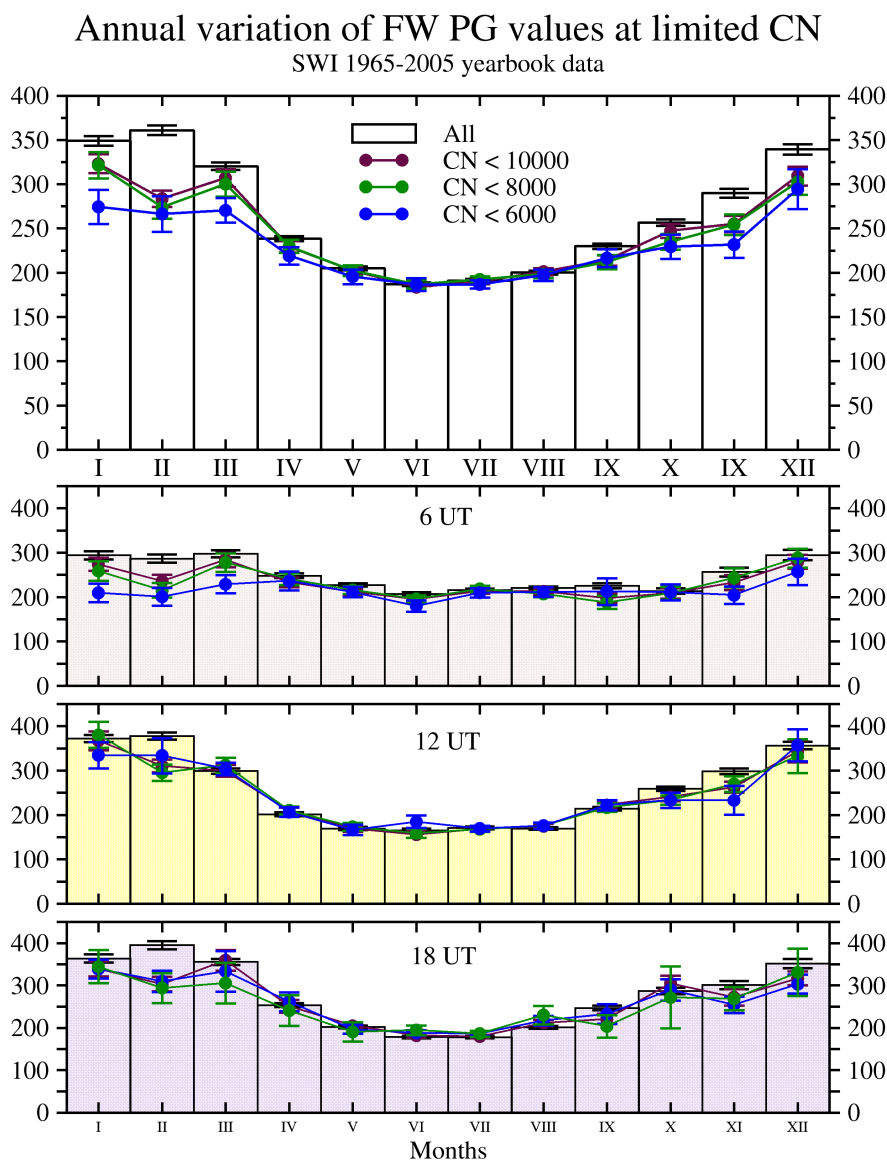
Figure 11. Annual variation of PG values measured during fair–weather conditions for all and limited CN concentration values for all hours (upper chart) and separately for each hour (6, 12, 18 UT). Error bars indicate one standard error of the mean.

Aerosol size observations show that polluted aerosol also occurs there and consists of large concentrations of fine particles dominated by the nuclei mode of the mean diameter 20–30 nm and the accumulated mode of the mean diameter 100–120 nm. Let us consider a mix of continental aerosol types the Świder aerosol may be composed of, and calculate the conductivities at 245 variable aerosol composition and concentrations. In the first place we want to focus on winter conditions when the decrease of

the potential gradient at lower CN concentrations, expected to be due to decreasing effect of pollution on the air conductivity, is the biggest as obtained in Sec. 4. Next we estimate the effect during the summer.

According to Hess et al. (1998) a land aerosol may consist of 3-4 main aerosol types: continental clean, continental average, continental polluted, and urban. These aerosol types consist of three basic aerosol components: water insoluble *(WatInsol)*,
250   water soluble *(WatSol)* and soot *(Soot)*, the two latest contributing almost 99 % of the total concentration and contained in the range of CN particle size. Their individual β coefficients are: $\beta_{WatInsol} = 2.80 \times 10^{-5}$ cm³/s, $\beta_{WatSol} = 1.18 \times 10^{-6}$ cm³/s, and $\beta_{Soot} = 5.56 \times 10^{-7}$ cm³/s, respectively, obtained from calculations based on the equations used in Tinsley and Zhou (2006). In this model the effect of relative humidity on the conductivity is not included.

$$\beta N = \beta_{WatInsol} N_{WatSol} + \beta_{WatSol} N_{WatSol} + \beta_{WatSol} N_{WatSol} \tag{3}$$

255

where $N_{WatInsol}$, N_{WatSol}, and N_{Soot} are number concentrations of the three aerosol components.

As a winter representative composition we choose a combination of the soot concentration up to 24000 cm⁻³ and the water soluble aerosol concentration up to 6000 cm⁻³ at different percentage ratio of water soluble – soot concentrations, and constant
260   concentration of water insoluble aerosol of $N_{WatInsol}$=500 cm⁻³. By increasing the concentration of water soluble aerosol we obtain mixes of aerosol of CN concentrations ranged from the seasonal average mean value (Fig. 4, Table 2) and the lowest considered limit of 6000 cm⁻³. This results also in variable ion conductivities. Table 5 presents the changes of the winter CN concentration, the ion-aerosol loss term, ion concentration and ion conductivity at different proportions of water soluble and soot aerosol components. The different proportions give the range of CN concentration between 6500 cm⁻³ (∼100 % of water
265   soluble aerosol) and 24500 cm⁻³ (∼100 % of soot). The air conductivity calculated from Eq. 1 is then between 2.28×10^{-15} S/m and 1.76×10^{-15} S/m.

As a summer representative composition we choose a combination of soot concentration up to 14000 cm⁻³ and water soluble aerosol concentration up to 6000 cm⁻³ at the different percentage ratio, in addition to the constant concentration of water insoluble aerosol at N=500 cm⁻³. The combinations give the range of CN concentrations between 6500 cm⁻³ (∼100 %
270   of water soluble aerosol) and 14500 cm⁻³ (∼100 % of soot), and the ion-loss term βN is calculated acording to Eq. 3. The air conductivity is then between 2.28× 10–15 S/m and 2.15× 10–15 S/m, as shown in Table 6.

The winter composition leading to the CN concentration of about 6000 cm⁻³ result in the ion conductivity 2.28×10^{-15} S/m, which is 1.3 the initial value of 1.76×10^{-15} S/m at 24500 cm⁻³ CN concentration, and the intermediate mixes give a monotonic increase of conductivity by 30 %. The summer case leading to the same low concentration of CN and the con-
275   ductivity of 2.28×10^{-15} S/m, which is 1.06 the initial conductivity of 2.18×10^{-15} S/m at 15500 cm⁻³. The intermediate mixes give an increase of conductivity by up to 6 % only. This should result in 30 % lower value of the PG according to Eq. 2 in the winter and 6 % decrease of the PG in the summer. Further, according to the model and Eq. 2, situations with low CN concentrations should result in at most 30 % decrease of the PG in the winter and up to 6 % decrease of the PG in the summer.

7 Discussion

280 At many land atmospheric electricity stations, including Świder, the increase of the potential gradient during local wintertime or rush hours, which is usually related to increase of emission from intensive domestic heating and transport, is considered to be due to a decrease in the electrical conductivity (Harrison, 2006; Kubicki et al., 2016; Tacza et al., 2021). Having at disposal all digitised PG hourly values we calculated the diurnal variation of PG from all available fair weather hours. As in the previous results of such analysis at Świder (e.g., Warzecha, 1991; Kubicki et al., 2007), made on the basis of 24-hour fair-

285 weather days 1965-2000, or fair weather hours during days with 12 hours of FW conditions over the time period 2004–2011 (Michnowski et al., 2021) the PG diurnal variation shown in Fig. 5 confirmed the different behaviour according to season. The double oscillation is evident during spring, summer and autumn (in the summer with peaks at 7 and 20 UT), and in winter a single oscillation (a minimum at ∼3UT and a peak at 19 UT). Similar PG diurnal curves were found in Reading for summer and winter (Nicoll et al., 2019). One hypothesis for the two PG peaks found in summer at urban sites could be due

290 to pollution of vehicular traffic during rush hours. Majewski and Przewoźniczuk (2009) performed Particulate Matter (10μm) measurements for eleven stations in Warsaw. They found clear two peaks (7 and 20 UT) in warm weather (April to September) and less pronounced peaks in cold weather (October to March). As mentioned earlier, Świder is located in a suburban site so vehicular transportation is not expected affect too much in the PG diurnal variation. Then, the hypothesis for the difference in the PG diurnal variation in summer and winter is a combination of "sunrise effect", generally thought to be related to mixing

295 of the near-surface electrode layer (which is an accumulation of positive charge next to the negatively charged Earth's surface). The first peak (at ∼7 UT) could be associated both with the dynamic changes in the planetary boundary layer and generation of the secondary aerosol.(Kubicki et al., 2007). Then, as the temperature is continuously increasing, the convection intensify producing mixing processes in the PBL causing transport of aerosol to higher altitudes and therefore, the PG decreases. As the temperature decrease after 16 UT the PG return to normal values. In winter, the reduced variability in PBL height (due

300 to diminished convection) therefore leads to more quiescent meteorological conditions which results in a more stable diurnal variation in PG, and the disappearance of the morning maximum peak (see also Nicoll et al., 2019).

The annual cycle of emissions with maxima in the winter and minima in the summer affecting the land PG measurements (Adlerman and Williams, 1996; Nicoll et al., 2019; Shatalina et al., 2019) are considerable at Świder, as confirmed in the analysis in Sec. 3 (Figs. 5, 6, 8). Similar behavior in the PG seasonal variation was found in Kew and Reading, in the UK,

305 and Nagycenk, in Hungary (Märcz et al., 1997; Harrison and Aplin, 2002; Nicoll et al., 2019). Harrison and Aplin (2002) associated the PG higher values during winter, at Kew, to the influence of smoke pollution. Märcz et al. (1997) suggested that the PG seasonal variation at Nagycenk is likely associated to the condensation nuclei variation. Nicoll et al. (2019) suggested that the PG higher values during winter at Reading is due to more use of domestic heating, and it is very likely that at Świder the PG values are higher during winter due to domestic heating producing soot. This is also in agreement with the simple

310 conductivity model in this work. Measurements of $PM_{2.5}$ in Krakow (south of Poland) found higher $PM_{2.5}$ concentrations during winter month compared with summer months for the period from 1 February 2020 to 27 March 2021 (Ryś and Samek,

2022). The time intervals of this study and the PG measurement at Świder are different (in fact both site locations are very far away), however, a similar behavior in PM is very likely at Świder.

The aerosol concentration changes also annually due to variation in convection processes in the planetary boundary layer
315 (PBL), and the PBL height, more influential during warm season and especially in the local summertime. At Świder, as discussed in Sec. 2.1, the summer CN concentrations differ much more from the rest of the year (Fig. 4) being minimal through all the year. As opposed to winter the change in the summer concentrations does not seem to be so significant on average (Fig. 9). The effect of reduced aerosol concentration to its lowest levels did not change the average PG amplitude in the summer, while in the other seasons this effect was observed particularly in the winter (Sec. 4).

320 According to the conductivity model for varying ground-level CN concentrations characteristic for Świder, described in Sec. 5, there could be ∼30 % decrease of the PG as a result to changes of the ion conductivity in the winter conditions with enhanced content of soot aerosol, and only a few percent decrease in the summer. The maximum decrease of the PG that we observe at the CN concentration of 6000 cm^{-3} in the winter is about 1.15 times and in the summer 1.03 times (see Table 3), which fairly agrees with the experimental model, itself not devoid of simplifications such as effects of humidity, constant ion
325 production. The differences between the model and observations should also arise from other factors affecting the PG such as, e.g., space charges, formation of secondary aerosol, or the conditions when the vertical particle current has other components than the conduction current, e.g. during convection etc. (e.g., Markson, 1975; Hoppel et al., 1986; Anisimov et al., 2017).

The changes of PG due to changes in the conductivity obscure the real changes of the PG resulting from the activity of the GEC, and the annual maximum of PG occurs usually during local winter. In this work we wanted to investigate in what way
330 taking into account fair weather PG values at low CN concentrations affects the PG annual maximum. In general, our results show that even though the PG decreases at low CN concentrations, ∼10 times more in the winter than in the summer (less than 10000, 8000, 6000 cm^{-3}) the maximum of PG remains in the winter. More recent analysis of the annual variation of PG in several places of different character of climate and pollution conditions show the PG maximum occurs in March and April.

8 Summary

335 The findings of this work could be summarised as follows:

- We calculated diurnal, seasonal and annual variations of fair-weather potential gradient based on 1965–2005 digitized time series of data from Świder observatory yearbooks, and we provided details of the statistics for the PG and the condensation nuclei CN number concentrations, measured during this period at three specific hours of measurement (6, 12 and 18 UT). The general average mean of PG is 230 V/m, and the average PG at the CN concentration observation
340 terms is 248 V/m while the CN average mean is about 19000 cm^{-3}. The PG and CN distributions are both leptokurtic (i.e., narrow) and right-skewed. A subset of PG values for CN concentration below 10000 cm^{-3} (which correspond to 20 % of the whole CN-PG pair data) was selected for further analysis of the effect of aerosol concentration on the PG variation. In particular, we aimed to investigate the PG annual variation in connection with the GEC variability. The PG

average mean for reduced levels of CN concentrations is 221 V/m, and the CN average mean isn this subset is 7290
345   cm^{-3}.

–   Summer and winter months have a clear signature in the PG diurnal variation for all CN concentrations, likely associated
    with mixing processes in the planetary boundary layer. For the subset with CN below $10000\ cm^{-3}$, we found that PG
    values do not show any significant variation in summer. On the other hand, for winter we found a big PG difference (11
    %). Furthermore, this PG difference is about 20% when we considered CN below $6000\ cm^{-3}$.

350   –   Local winter months have higher PG values compared with local summer months, a common feature of continental
    atmospheric electricity stations. Furthermore, this PG seasonal variation is maintained even at lower CN concentrations
    (e.g., 10000, 8000, $6000\ cm^{-3}$). We found that there is a reduction in the PG values by 11-26 % with the biggest
    difference in February. In summer months, this difference is negligible. From this, we can conclude that aerosol at these
    concentrations has more effect in the PG during winter compared with summer.

355   –   A simplified modelling of electrical conductivity affecting the PG is created. The ion loss in this model is due to at-
    tachment mainly to water soluble aerosol particles and soot particles, the main components of continental aerosol. At
    different percentage ratios of these two components leading to low total concentration of CN (down to $6500\ cm^{-3}$) we
    obtain changes in the conductivity and the PG in fair agreement with observations up to 30 % in the winter, and 6 % in
    the summer.

360   –   Despite our efforts to minimise the aerosol effect on the PG (through CN concentration measurements), the character
    of the PG seasonal and annual variation does not radically changes, with the maximum remaining in the winter and the
    minimum in the summer (Northern Hemisphere winter and summer).

Data availability. Data is available on request from co-author A. Odzimek (aodzimek@igf.edu.pl).

Appendix A

365   This Appendix contains the list of Świder Observatory yearbooks used in this study.

Warzecha S. (Ed.), 1968: Rocznik Elektryczności Atmosferycznej i Meteorologii 1965, Prace Obs. Geof. Świder 38.

Warzecha S. (Ed.), 1968: Électricité atmosphérique et météorologie Observatoire Géophysique de St. Kalinowski à Świder
1966, Mater. Prace Zakł. Geofizyki 23.

370   Warzecha S. (Ed.), 1969: Électricité atmosphérique et météorologie Observatoire Géophysique de St. Kalinowski à Świder
1967, Mater. Prace Zakł. Geofizyki 28.

Warzecha S. (Ed.), 1970: Électricité atmosphérique et météorologie Observatoire Géophysique de St. Kalinowski à Świder
1968, Mater. Prace Zakł. Geofizyki 38.

Warzecha S. (Ed.), 1971: Électricité atmosphérique et météorologie Observatoire Géophysique de St. Kalinowski à Świder

375   1969, Mater. Prace Zakł. Geofizyki 44.

Warzecha S. (Ed.), 1972: Électricité atmosphérique et météorologie Observatoire Géophysique de St. Kalinowski à Świder
1970, Mater. Prace Zakł. Geofizyki 53.

Warzecha S. (Ed.), 1973: Électricité atmosphérique et météorologie Observatoire Géophysique de St. Kalinowski à Świder
1971, Mater. Prace Zakł. Geofizyki 63.

380   Warzecha S. (Ed.), 1974: Électricité atmosphérique et météorologie Observatoire Géophysique de St. Kalinowski à Świder
1972, Mater. Prace Zakł. Geofizyki 77.

Warzecha S. (Ed.), 1974: Électricité atmosphérique et météorologie Observatoire Géophysique de St. Kalinowski à Świder
1973, Mater. Prace Zakł. Geofizyki 80.

Warzecha S. (Ed.), 1975: Électricité atmosphérique et météorologie Observatoire Géophysique de St. Kalinowski à Świder

385   1974, Mater. Prace Zakł. Geofizyki 92.

Warzecha S. (Ed.), 1976: Électricité atmosphérique et météorologie Observatoire Géophysique de S. Kalinowski à Świder
1975, Publs. Inst. Geophys. Pol. Acad. Sci., 104(D-2).

Warzecha S. (Ed.), 1978: Électricité atmosphérique et météorologie Observatoire Géophysique de S. Kalinowski à Świder
1976, Publs. Inst. Geophys. Pol. Acad. Sci., 121(D-6).

390   Warzecha S. (Ed.), 1979: Électricité atmosphérique et météorologie Observatoire Géophysique de S. Kalinowski à Świder
1977, Publs. Inst. Geophys. Pol. Acad. Sci., 131(D-8).

Warzecha S. (Ed.), 1980: Électricité atmosphérique et météorologie Observatoire Géophysique de S. Kalinowski à Świder
1978, Publs. Inst. Geophys. Pol. Acad. Sci., 140(D-10).

Warzecha S. (Ed.), 1981: Électricité atmosphérique et météorologie Observatoire Géophysique de S. Kalinowski à Świder

395   1979, Publs. Inst. Geophys. Pol. Acad. Sci., 148(D-12).

Warzecha S. (Ed.), 1982: Électricité atmosphérique et météorologie Observatoire Géophysique de S. Kalinowski à Świder
1980, Publs. Inst. Geophys. Pol. Acad. Sci., 151(D-14).

Warzecha S. (Ed.), 1982: Électricité atmosphérique et météorologie Observatoire Géophysique de S. Kalinowski à Świder
1981, Publs. Inst. Geophys. Pol. Acad. Sci., 158(D-16).

400   Warzecha S. (Ed.), 1983: Électricité atmosphérique et météorologie Observatoire Géophysique de S. Kalinowski à Świder
1982, Publs. Inst. Geophys. Pol. Acad. Sci., 168(D-17).

Warzecha S. (Ed.), 1984: Électricité atmosphérique et météorologie Observatoire Géophysique de S. Kalinowski à Świder
1983, Publs. Inst. Geophys. Pol. Acad. Sci., 177(D-19).

Warzecha S. (Ed.), 1985: Électricité atmosphérique et météorologie Observatoire Géophysique de S. Kalinowski à Świder

405   1984, Publs. Inst. Geophys. Pol. Acad. Sci., 190(D-23).

Warzecha S. (Ed.), 1986: Électricité atmosphérique et météorologie Observatoire Géophysique de S. Kalinowski à Świder
1984, Publs. Inst. Geophys. Pol. Acad. Sci., 194(D-24).

Warzecha S. (Ed.), 1987: Électricité atmosphérique et météorologie Observatoire Géophysique de S. Kalinowski à Świder

1985, Publs. Inst. Geophys. Pol. Acad. Sci., 209(D-27).

410 Warzecha S. (Ed.), 1988: Électricité atmosphérique et météorologie Observatoire Géophysique de S. Kalinowski à Świder
1984, Publs. Inst. Geophys. Pol. Acad. Sci., 219(D-29).

Warzecha S. (Ed.), 1989: Électricité atmosphérique et météorologie Observatoire Géophysique de S. Kalinowski à Świder
1988, Publs. Inst. Geophys. Pol. Acad. Sci., 229(D-31).

Warzecha S. (Ed.), 1990: Électricité atmosphérique et météorologie Observatoire Géophysique de S. Kalinowski à Świder

415 1989, Publs. Inst. Geophys. Pol. Acad. Sci., 234(D-34).

Warzecha S. (Ed.), 1991: Électricité atmosphérique et météorologie Observatoire Géophysique de S. Kalinowski à Świder
1990, Publs. Inst. Geophys. Pol. Acad. Sci., 247(D-37).

Warzecha S. (Ed.), 1992: Électricité atmosphérique et météorologie Observatoire Géophysique de S. Kalinowski à Świder
1991, Publs. Inst. Geophys. Pol. Acad. Sci., 253(D-39).

420 Warzecha S. (Ed.), 1993: Électricité atmosphérique et météorologie Observatoire Géophysique de S. Kalinowski à Świder
1992, Publs. Inst. Geophys. Pol. Acad. Sci., 264(D-41).

Warzecha S. (Ed.), 1994: Électricité atmosphérique et météorologie Observatoire Géophysique de S. Kalinowski à Świder
1993, Publs. Inst. Geophys. Pol. Acad. Sci., 271(D-43).

Warzecha S. (Ed.), 1995: Électricité atmosphérique et météorologie Observatoire Géophysique de S. Kalinowski à Świder

425 1994, Publs. Inst. Geophys. Pol. Acad. Sci., 280(D-44).

Warzecha S. (Ed.), 1996: Électricité atmosphérique et météorologie Observatoire Géophysique de S. Kalinowski à Świder
1995, Publs. Inst. Geophys. Pol. Acad. Sci., 290(D-47).

Kubicki M. (Ed.), 1997: Results of atmospheric electricity and meteorological observations. S.Kalinowski Geophysical Observatory at Świder - 1996, Publs. Inst. Geophys. Pol. Acad. Sci., 299(D-49).

430 Kubicki M. (Ed.), 1998: Results of atmospheric electricity and meteorological observations. S.Kalinowski Geophysical Observatory at Świder - 1997, Publs. Inst. Geophys. Pol. Acad. Sci., 307(D-51).

Kubicki M. (Ed.), 1999: Results of atmospheric electricity and meteorological observations. S.Kalinowski Geophysical Observatory at Świder - 1998, Publs. Inst. Geophys. Pol. Acad. Sci., 321(D-52).

Kubicki M. (Ed.), 2000: Results of atmospheric electricity and meteorological observations. S.Kalinowski Geophysical Observatory at Świder - 1999, Publs. Inst. Geophys. Pol. Acad. Sci., 324(D-54).

435 Kubicki M. (Ed.), 2001: Results of atmospheric electricity and meteorological observations. S.Kalinowski Geophysical Observatory at Świder - 2000, Publs. Inst. Geophys. Pol. Acad. Sci., 333(D-55).

Kubicki M. (Ed.), 2002: Results of atmospheric electricity and meteorological observations. S.Kalinowski Geophysical Observatory at Świder - 2001, Publs. Inst. Geophys. Pol. Acad. Sci., 342(D-58).

440 Kubicki M. (Ed.), 2003: Results of atmospheric electricity and meteorological observations. S.Kalinowski Geophysical Observatory at Świder - 2002, Publs. Inst. Geophys. Pol. Acad. Sci., 355(D-61).

Kubicki M. (Ed.), 2004: Results of atmospheric electricity and meteorological observations. S.Kalinowski Geophysical Observatory at Świder - 2003, Publs. Inst. Geophys. Pol. Acad. Sci., 372(D-65).

Kubicki M. (Ed.), 2005: Results of atmospheric electricity and meteorological observations. S.Kalinowski Geophysical Observatory at Świder - 2004, Publs. Inst. Geophys. Pol. Acad. Sci., 383(D-68).

Kubicki M. (Ed.), 2006: Results of atmospheric electricity and meteorological observations. S.Kalinowski Geophysical Observatory at Świder - 2005, Publs. Inst. Geophys. Pol. Acad. Sci., 391(D-71).

Appendix B

This Appendix contains the list of additional Tables: Table B1, Table B2 and Table B3.

Author contributions. AO digitised PG and CN data from Świder yearbooks and conceived the subject of the study. IZ and AO performed the investigation and wrote the paper. DK and JT revised and edited the paper. All authors discussed the results.

Competing interests. The authors declare that they have no competing interests.

Acknowledgements. The work is supported by Poland National Science Centre grant No 2021/41/B/ST10/04448 at the Institute of Geophysics, Polish Academy of Sciences.

References

Adlerman, E. J. and Williams, E. R.: Seasonal variation of the global electrical circuit, J. Geophys. Res.-Atmos., 101, 29 679–29 688, https://doi.org/10.1029/96JD01547, 1996.

Anisimov, S., Galichenko, S., and Mareev, E.: Electrodynamic properties and height of atmospheric convective boundary layer, Atmos. Res., 194, 119–129, https://doi.org/https://doi.org/10.1016/j.atmosres.2017.04.012, 2017.

Bennett, A. J. and Harrison, R. G.: Variability in surface atmospheric electric field measurements, Journal of Physics: Conference Series, 142, 012 046, https://doi.org/10.1088/1742-6596/142/1/012046, 2008.

Christian, H. J., Blakeslee, R. J., Boccippio, D. J., Boeck, W. L., Buechler, D. E., Driscoll, K. T., Goodman, S. J., Hall, J. M., Koshak, W. J., Mach, D. M., and Steward, D. F.: Global frequency and distribution of lightning as observed from space by the Optical Transient Detector, J. Geophys. Res.-Atmos., 108, ACL 4–1–ACL 4–15, https://doi.org/10.1029/2002JD002347, 2003.

Harrison, R.: Urban smoke concentrations at Kew, London, 1898–2004, Atmospheric Environment, 40, 3327–3332, https://doi.org/https://doi.org/10.1016/j.atmosenv.2006.01.042, 2006.

Harrison, R. and Aplin, K.: Mid-nineteenth century smoke concentrations near London, Atmos. Env., 36, 4037–4043, https://doi.org/https://doi.org/10.1016/S1352-2310(02)00334-5, 2002.

Harrison, R. G.: The Carnegie Curve, Surv. Geophys., 34, 209–232, https://doi.org/10.1007/s10712-012-9210-2, 2013.

Hess, M., Koepke, P., and Schult, I.: Optical Properties of Aerosols and Clouds: The Software Package OPAC, Bulletin of the American Meteorological Society, 79, 831 – 844, https://doi.org/10.1175/1520-0477(1998)079<0831:OPOAAC>2.0.CO;2, 1998.

Hoffmann, K.: Bericht uber die in Ebeltofthafen auf Spitsbergen in der Jahren 1913/14 durchgefurten luftelektrischen Messungen (11 36' 15" E, 79 09' 14" N), Breitr. Phys. Frei. Atmos., 11, 1–19, Report about the Atmospheric Electric Measurements Performed in 1913/14 in Ebeltolthafen in Spitsberegen (11 36' 15" E, 79 09' 14" N), 1924.

Hoppel, W. A., Anderson, R. V., and Willett, J. C.: Atmospheric electricity in the planetary boundary layer, pp. 149–165, Natl. Acad. Press, Washington, D.C., 1986.

Imyanitov, I. M. and Chubarina, Y. V.: Electricity of free atmosphere, Gidrometeoizdat, Leningrad, 1965, Technical Translation from Russian, NASA, Washington, TT F-425, 1967.

Israël, H.: Atmospheric Electricity, vol. I, Fundamentals, Conductivity, Ions, Israel Program for Scientific Translations, Jerusalem, 1973a.

Israël, H.: Atmospheric Electricity, vol. II, Fields, Charges, Currents, Israel Program for Scientific Translations, Jerusalem, 1973b.

Kubicki, M.: Results of Atmospheric Electricity and Meteorological Observations at S. Kalinowski Geophysical Observatory at Świder, 2005, Publ. Inst. Geophys. Pol. Acad. Sci., 391(D-71), 3–27, 2006.

Kubicki, M., Michnowski, S., Myslek-Laurikainen, B., and Warzecha, S.: Long term variations of some atmospheric electricity, aerosol, and extraterrestrial parameters at Swider Observatory, Poland, in: Proceedings of the 12th International Conference on Atmospheric Electricity, 9-13 June 2003, Versailles, France, pp. 291–294, 2003.

Kubicki, M., Michnowski, S., and Myslek-Laurikainen, B.: Seasonal and daily variations of atmospheric electricity parameters registered at the Geophysical Observatory at Świder (Poland) during 1965-2000, in: Proceedings of the 13th International Conference on Atmospheric Electricity, 13-17 August 2007, Beijing, China, vol. I, p. 4 pp., 2007.

Kubicki, M., Odzimek, A., and Neska, M.: Relationship of ground-level aerosol concentration and atmospheric electric field at three observation sites in the Arctic, Antarctic and Europe, Atmos. Res., 178-179, 329–346, https://doi.org/10.1016/j.atmosres.2016.03.029, 2016.

Majewski, G. and Przewoźniczuk, W.: Study of Particulate Matter Pollution in Warsaw Area, Pol. J. Environ Studies, 18, 293–300, https://www.pjoes.com/Study-of-Particulate-Matter-Pollution-r-nin-Warsaw-Area,88234,0,2.html, 2009.

Markson, R.: Atmospheric Electrical Detection of Organized Convection, Science, 188, 1171–1177,
495   https://doi.org/10.1126/science.188.4194.1171, 1975.

Matthews, J., Wright, M., Clarke, D., Morley, E., Silva, H., Bennett, A., Robert, D., and Shallcross, D.: Urban and rural measurements of atmospheric potential gradient, Journal of Electrostatics, 97, 42–50, https://doi.org/https://doi.org/10.1016/j.elstat.2018.11.006, 2019.

Michnowski, S., Odzimek, A., Kleimenova, N. G., Kozyreva, O. V., Kubicki, M., Klos, Z., Israelsson, S., and Nikiforova, N. N.: Review of Relationships Between Solar Wind and Ground-Level Atmospheric Electricity: Case Studies from Hornsund, Spitsbergen, and Swider,
500   Poland, Surv. Geophys., 42, 757–801, https://doi.org/10.1007/s10712-021-09639-3, 2021.

Mohnen, V. and Hidy, G. M.: Measurements of Atmospheric Nanoparticles (1875–1980), Bull. Amer. Meteorol. Soc., 91, 1525 – 1540, https://doi.org/10.1175/2010BAMS2929.1, 2010.

Märcz, F., Sátori, G., and Zieger, B.: Variations in Schumann resonances and their relation to atmospheric electric parameters at Nagycenk station, Ann. Geophys., 15, 1604–1614, https://doi.org/10.1007/s00585-997-1604-y, 1997.

505 Nicoll, K., Harrison, R., Barta, V., Bor, J., Brugge, R., Chillingarian, A., Chum, J., Georgoulias, A., Guha, A., Kourtidis, K., Kubicki, M., Mareev, E., Matthews, J., Mkrtchyan, H., Odzimek, A., Raulin, J.-P., Robert, D., Silva, H., Tacza, J., Yair, Y., and Yaniv, R.: A global atmospheric electricity monitoring network for climate and geophysical research, J. Atmos. Sol.-Terr. Phys., 184, 18–29, https://doi.org/10.1016/j.jastp.2019.01.003, 2019.

Odzimek, A.: Polar regions in the Earth's global atmospheric electric circuit research, Prz. Geof., 64, 35–72, https://doi.org/10.32045/PG-
510   2019-002, 2019.

Parkinson, W. L. and Torreson, O. W.: The diurnal variation of the electric potential of the atmosphere over the oceans, Union Terr. Magn. Electr. Bull., 8, 340–341, 1931.

Pietruczuk, A. and Jarosławski, J.: Analysis of particulate matter concentrations in Mazovia region, Central Poland, based on 2007–2010 data, Acta Geophys., 61, 445–462, https://doi.org/10.2478/s11600-012-0069-x, 2013.

515 Rycroft, M. J., Israelsson, S., and Price, C.: The global atmospheric electric circuit, solar activity and climate change, J. Atmos. Sol.-Terr. Phys., 62, 1563–1576, https://doi.org/10.1016/S1364-6826(00)00112-7, 2000.

Ryś, A. and Samek, L.: Yearly Variations of Equivalent Black Carbon Concentrations Observed in Krakow, Poland, Atmosphere, 13, 539, https://doi.org/10.3390/atmos13040539, 2022.

Shatalina, M. V., Mareev, E. A., Klimenko, V. V., Kuterin, F. A., and Nicoll, K. A.: Experimental Study of Diurnal and Seasonal Variations
520   in the Atmospheric Electric Field, Radiophys. Quant. Electr., 62, 183–191, https://doi.org/10.1007/s11141-019-09966-x, 2019.

Tacza, J., Raulin, J.-P., Macotela, E., Marun, A., Fernandez, G., Bertoni, F., Lima, L., Samanes, J., Buleje, Y., Correia, E., Alves, G., and Makita, K.: Local and global effects on the diurnal variation of the atmospheric electric field in South America by comparison with the Carnegie curve, Atmos. Res., 240, 104 938, https://doi.org/10.1016/j.atmosres.2020.104938, 2020.

Tacza, J., Raulin, J. P., Morales, C. A., Macotela, E., Marun, A., and Fernandez, G.: Analysis of long-term potential gradient variations
525   measured in the Argentinian Andes, Atmos. Res., 248, 105200, https://doi.org/10.1016/j.atmosres.2020.105200, 2021.

Tinsley, B. A. and Zhou, L.: Initial results of a global circuit model with variable stratospheric and tropospheric aerosols, J. Geophys. Res.-Atmos., 111, D16 205, https://doi.org/10.1029/2005JD006988, 2006.

Warzecha, S., ed.: Annuaire Meteorologique et de l'electricite atmospherique 1957, vol. 16 of *Travaux de l'Observatoire Géophysique de St. Kalinowski à Świder*, 1960.

530 Warzecha, S., ed.: Annuaire Meteorologique et de l'electricite atmospherique 1965, vol. 38 of *Travaux de l'Observatoire Géophysique de St. Kalinowski à Świder*, 1968.

Warzecha, S.: Wpływ czynników meteorologicznych na koncentrację atmosferycznych jąder kondensacji w Świdrze., Phd thesis, Instytut Geofizyki, Polska Akademia Nauk, 1974.

Warzecha, S.: Periodical variations of the condensation nuclei content at Świder, Publs. Inst. Geophys. Pol. Acad. Sci., 99, 17–35, 1976.

535 Warzecha, S.: Variations of the Electric Field and air conductivity at Swider in the years 1958-1985, Publs. Inst. Geophys. Pol. Acad. Sci., 238, 193pp., 1991.

Witkowski, A.: Spostrzeżenia nad elektrycznością atmosferyczną w Zakopanem. (Note sur l'électricité atmosphérique à Zakopane dans les Tatras), Bull. Acad. Sci. Cracovie A, 42, 7–10, 1902.

Wright, M., Matthews, J., Silva, H., Bacak, A., Percival, C., and Shallcross, D.: The relationship between aerosol
540 concentration and atmospheric potential gradient in urban environments, Sci. Total Environ., 716, 134959, https://doi.org/https://doi.org/10.1016/j.scitotenv.2019.134959, 2020.

Table 4. Mean values of PG measured for fair–weather conditions by month for all and limited CN concentration values together with the standard deviation of the mean value corresponding to 6, 12, 18 UT.

Hour	PG (V/m)	Jan	Feb	Mar	Apr	May	Jun	Jul	Aug	Sep	Oct	Nov	Dec
All	CN all	349±5	361±5	320±4	239±3	205±2	187±2	191±2	200±2	230±3	257±4	290±5	339±6
	CN<10000	323±11	283±9	307±10	229±7	202±4	184±4	190±3	201±4	214±6	247±8	255±9	309±11
	CN<8000	321±15	274±13	300±14	230±8	202±6	187±5	192±4	198±5	212±8	235±9	254±12	303±14
	CN<6000	274±19	266±20	270±14	219±10	195±8	187±7	187±5	197±6	216±10	229±14	232±15	294±22
6 UT	CN all	294±9	286±9	298±8	248±5	227±4	207±4	216±3	220±4	226±6	213±6	256±10	295±11
	CN<10000	273±15	236±14	283±16	233±10	211±6	195±5	213±5	212±6	197±10	208±12	232±17	279±15
	CN<8000	258±22	215±16	277±20	240±13	215±9	195±7	218±7	206±6	188±15	208±14	243±21	287±21
	CN<6000	209±20	200±20	228±20	236±21	211±11	179±12	209±10	211±10	212±30	210±18	204±19	256±29
12 UT	CN all	372±8	378±8	298±6	202±4	170±4	165±4	171±3	170±3	214±4	259±5	298±7	356±9
	CN<10000	367±21	310±14	299±13	208±7	169±7	155±7	168±4	174±5	222±7	240±9	262±12	343±24
	CN<8000	380±29	295±18	311±17	210±9	173±8	158±10	167±5	175±6	216±9	233±10	269±17	332±37
	CN<6000	334±29	333±39	303±13	206±10	166±11	184±13	169±6	175±7	221±11	233±17	233±32	357±36
18 UT	CN all	364±10	395±10	355±7	253±5	202±3	178±3	178±3	201±3	247±6	287±8	301±10	351±11
	CN<10000	339±17	303±17	359±24	250±15	205±6	181±5	179±4	211±7	221±12	304±18	271±19	316±16
	CN<8000	338±22	309±24	333±48	261±22	196±10	188±6	186±5	216±11	232±23	289±25	254±19	303±22
	CN<6000	344±38	293±35	305±47	240±35	190±22	194±11	185±7	229±21	203±26	271±73	268±27	331±55

Table 5. Model of winter CN concentration, the ion-aerosol loss term βN, and ion conductivity at different aerosol composition of water soluble particles and soot components.

Soot (%)	WatSol (%)	CN (cm^{-3})	βN (cm^3/s)	Conductivity (S/m)	s
100	0	24500	1.12E-06	1.76E-15	1.00
90	10	22700	1.18E-06	1.80E-15	1.02
80	20	20900	1.25E-06	1.84E-15	1.05
70	30	19100	1.33E-06	1.89E-15	1.07
60	40	17300	1.44E-06	1.93E-15	1.10
50	50	15500	1.56E-06	1.98E-15	1.13
40	60	13700	1.72E-06	2.04E-15	1.16
30	70	11900	1.93E-06	2.09E-15	1.19
20	80	10100	2.21E-06	2.15E-15	1.22
10	90	8300	2.62E-06	2.21E-15	1.26
0	100	6500	3.24E-06	2.28E-15	1.30

Table 6. Model of summer CN concentration, the ion-aerosol loss term βN, and ion conductivity at different aerosol composition of water soluble and soot components.

Soot (%)	WatSol (%)	CN (cm^{-3})	βN (cm^3/s)	Conductivity (S/m)	s
100	0	14500	1.50E-06	2.15E-15	1.00
90	10	13700	1.58E-06	2.16E-15	1.00
80	20	12900	1.68E-06	2.18E-15	1.01
70	30	12100	1.78E-06	2.19E-15	1.01
60	40	11300	1.90E-06	2.20E-15	1.01
50	50	10500	2.04E-06	2.21E-15	1.02
40	60	9700	2.20E-06	2.23E-15	1.02
30	70	8900	2.39E-06	2.24E-15	1.02
20	80	8100	2.62E-06	2.25E-15	1.03
10	90	7300	2.90E-06	2.27E-15	1.03
0	100	6500	3.24E-06	2.28E-15	1.06

Table B1. Number of hourly values of PG at fair-weather hours divided into months for January 1965 – December 2005. Last column indicates the number of hours without PG measurements.

Season	Winter			Spring			Summer			Autumn			total	missing
Y\M	Dec	Jan	Feb	Mar	Apr	May	Jun	Jul	Aug	Sep	Oct	Nov		
1965	105	211	148	315	205	275	286	342	332	440	270	58	2987	59
1966	125	85	193	226	340	289	462	391	476	407	324	99	3417	91
1967	104	242	268	256	288	383	370	443	445	395	385	222	3801	152
1968	138	100	146	340	427	342	384	339	529	364	244	116	3469	109
1969	181	257	177	308	346	361	401	374	354	394	235	110	3498	111
1970	31	199	197	152	224	271	410	297	324	203	91	113	2512	24
1971	33	275	106	241	309	404	300	512	526	221	207	143	3277	99
1972	300	214	276	279	200	320	347	433	237	149	251	127	3133	68
1973	174	184	46	346	287	311	326	273	552	305	209	181	3194	107
1974	104	236	217	501	347	239	261	201	432	376	150	207	3271	142
1975	137	195	204	256	191	339	309	373	473	430	167	182	3256	103
1976	94	124	321	178	281	321	318	397	382	289	199	140	3044	64
1977	96	252	98	291	227	299	390	304	287	281	189	146	2860	68
1978	129	237	120	230	271	374	351	268	143	67	69	41	2300	14
1979	128	45	237	150	233	401	290	119	171	156	346	63	2339	110
1980	95	126	86	242	190	247	167	90	181	143	179	99	1845	47
1981	109	102	165	225	228	309	229	243	277	185	132	35	2239	87
1982	21	129	158	316	136	383	230	373	408	361	239	200	2954	98
1983	126	60	131	180	264	271	359	356	461	253	150	89	2700	67
1984	56	63	259	281	346	279	130	234	441	149	275	156	2669	87
1985	70	164	153	124	326	399	205	358	373	176	89	76	2513	42
1986	108	95	303	295	323	421	351	311	334	146	259	136	3082	85
1987	69	212	147	292	208	284	182	343	288	288	431	132	2876	80
1988	84	174	168	187	409	328	286	419	370	203	403	171	3202	42
1989	156	75	152	262	256	425	201	403	296	346	145	64	2781	54
1990	106	119	208	264	318	355	328	282	392	174	320	25	2891	82
1991	128	197	123	165	309	311	281	405	333	422	291	183	3148	73
1992	224	166	100	275	243	391	470	485	543	459	195	174	3725	74
1993	119	326	164	366	401	517	411	398	427	252	274	157	3812	56
1994	104	178	225	169	373	407	380	614	378	245	248	231	3552	81
1995	184	156	244	174	317	352	341	553	496	188	185	161	3351	42
1996	304	302	220	272	456	279	398	329	447	186	247	227	3667	152
1997	155	191	221	370	331	373	334	285	536	319	219	180	3514	65
1998	172	281	222	379	290	405	297	312	274	342	265	146	3385	243
1999	202	220	110	360	303	442	271	471	434	478	259	214	3764	79
2000	137	123	221	200	444	543	464	265	426	425	595	265	4108	100
2001	143	156	245	310	255	479	335	316	511	232	249	171	3402	90
2002	273	158	336	370	348	491	398	441	525	377	180	289	4186	39
2003	298	216	277	314	352	482	382	373	501	455	186	166	4002	50
2004	180	153	162	221	431	319	333	415	463	453	292	187	3609	25
2005	41	219	233	356	428	453	390	430	536	552	455	206	4299	42
total	5543	7217	7787	11038	12461	14874	13358	14570	16314	12286	10098	6088	131634	3303
	20547			38373			44242			28472				

Table B2. Number of fair-weather days (24h) divided into months for the period January 1965 – December 2005.

| Season | Winter | | | Spring | | | Summer | | | Autumn | | | total |
Y\M	Dec	Jan	Feb	Mar	Apr	May	Jun	Jul	Aug	Sep	Oct	Nov	
1965	–	2	–	3	–	4	3	5	6	10	2	–	35
1966	–	–	3	1	5	5	11	1	11	4	2	–	43
1967	1	4	3	1	3	10	3	6	2	7	3	3	46
1968	1	–	1	3	10	–	6	3	7	4	2	2	39
1969	3	5	1	4	6	5	3	7	5	8	1	–	48
1970	–	2	1	1	2	4	6	1	5	2	–	–	24
1971	–	2	–	1	5	4	3	12	11	3	2	–	43
1972	4	4	6	6	2	3	5	9	2	1	1	–	43
1973	1	3	–	3	2	4	5	1	11	2	1	1	34
1974	–	4	3	11	4	2	1	–	10	6	–	2	43
1975	–	3	1	3	1	2	3	7	12	6	4	1	43
1976	–	2	6	1	1	5	7	7	5	4	1	–	39
1977	2	2	–	2	1	2	5	4	4	2	1	1	26
1978	–	5	1	2	3	7	5	1	1	–	–	–	25
1979	–	–	3	–	3	3	2	–	2	–	3	–	16
1980	1	–	–	–	2	–	–	–	–	–	–	–	3
1981	–	–	1	1	3	2	1	1	3	–	–	–	12
1982	–	–	–	4	–	10	4	2	6	2	3	2	33
1983	–	–	–	3	2	1	3	2	7	3	–	–	21
1984	–	–	5	3	3	1	–	3	5	–	1	2	23
1985	–	2	1	–	3	7	1	–	5	–	–	–	19
1986	1	–	6	4	5	6	2	3	3	1	2	–	33
1987	–	1	1	6	1	3	1	4	4	2	7	–	30
1988	1	2	1	–	7	3	2	5	1	1	6	3	32
1989	1	–	–	2	3	7	1	7	2	5	–	–	28
1990	–	–	–	4	6	6	1	2	6	–	2	–	27
1991	–	1	–	1	3	3	1	6	2	4	3	–	24
1992	2	–	–	3	1	5	4	9	9	10	1	–	44
1993	–	6	–	5	8	7	7	4	6	2	3	1	49
1994	–	2	1	–	2	3	7	16	2	–	3	4	40
1995	1	1	–	–	4	3	3	10	7	–	–	–	29
1996	2	4	–	1	6	–	9	–	5	1	2	1	31
1997	1	–	1	3	2	6	3	–	13	3	1	3	36
1998	1	2	–	5	1	5	4	3	3	4	2	1	31
1999	1	1	–	6	4	6	3	9	2	10	2	2	46
2000	1	–	1	–	6	12	8	1	5	6	16	1	57
2001	–	–	1	–	3	6	1	–	6	1	1	–	19
2002	–	–	3	6	2	6	5	8	14	5	–	3	52
2003	4	1	4	6	4	8	6	3	5	6	–	–	47
2004	2	–	3	1	10	2	1	3	3	5	4	–	34
2005	–	2	4	5	4	9	–	5	10	15	11	2	67
total	31	63	62	111	143	187	146	170	228	145	93	35	1414
		156			441			544			273		

Table B3. Number of PG values measured in FW conditions by month for all and limited CN concentrations corresponding to 6, 12, 18 UT.

Hour	PG length	Jan	Feb	Mar	Apr	May	Jun	Jul	Aug	Sep	Oct	Nov	Dec
6UT	all CN	239	269	418	545	737	653	702	754	475	347	190	190
	PG with all CN	236	258	397	526	709	628	670	723	449	326	178	183
	CN<10000	52	45	63	102	240	217	242	218	88	55	50	55
	CN<8000	27	25	37	52	139	118	138	123	36	34	3 5	34
	CN<6000	16	13	22	21	56	45	58	55	9	13	18	18
12 UT	all CN	363	388	467	382	409	329	377	523	481	508	336	301
	PG with all CN	356	377	453	374	395	322	367	514	476	497	329	298
	CN<10000	41	47	55	76	79	74	137	160	109	94	56	35
	CN<8000	20	25	31	63	51	44	108	110	72	52	25	16
	CN<6000	8	7	19	42	27	25	73	72	36	17	9	8
18 UT	all CN	322	393	544	621	718	676	713	772	599	467	293	255
	PG with all CN	318	377	526	592	682	638	671	722	564	418	277	246
	CN<10000	47	44	36	54	153	222	270	166	65	48	43	55
	CN<8000	29	26	14	22	70	123	151	79	25	18	25	28
	CN<6000	8	14	8	8	19	49	65	23	12	4	13	5